Data Assimilation for Prediction of Surrounding Rock Mass Behavior during Underground Structure Construction Phases

Yasuhisa Aono
Shimizu Corporation, Tokyo, Japan

Tetsuo Okuno
Shimizu Corporation, Tokyo, Japan

ABSTRACT: To ensure safety during the construction of underground structures, the present and future conditions of rock and tunnel supports, such as displacements, stresses, and plastic regions, must be estimated and predicted by appropriate measurements and numerical simulations. However, there are many uncertainties, such as geological structures, mechanical properties of rocks, and initial and boundary conditions, which considerably complicate numerical modeling. To solve this problem, this study develops a numerical analysis method using a data assimilation (DA) technique that updates the numerical model based on the measured data during construction. Numerical experiments were conducted to evaluate the effectiveness of the proposed method. DA analyses were performed using the displacements obtained from the simulated measurement data. As a result, DA updated the physical properties of the elasto-plastic model and improved the prediction performance of the displacements and plastic region of the surrounding rock mass during tunnel construction.

Keywords: Ensemble-based data assimilation, Underground structures, Numerical analysis, Strain softening.

1 INTRODUCTION

In the construction of underground structures such as mountain tunnels and underground power plants, tunnel face observations and ground displacement measurements are conducted daily to evaluate the surrounding rock mass behavior of those structures. Based on the results of observations and measurements, the original support design and construction methods are modified to suit actual ground conditions. The design and construction methods are modified based on past cases. Numerical analysis is occasionally performed when unexpected phenomena occur or are foreseen, such as excessive ground deformation or instability of the tunnel face. However, many uncertainties, such as geological structures, mechanical properties of rocks, and initial and boundary conditions, considerably complicate numerical modeling.

Previous studies examined methods for predicting ground properties and displacements through analysis using measurement data obtained during tunnel construction. Moreover, research has been conducted on methods for predicting the behavior of embankments using data assimilation (DA) by

Shuku et al. (2011). According to this report, the advantage of DA is that the probability distribution of the analysis results can be evaluated. Because the ground is heterogeneous and its mechanical properties are uncertain, we believe that the predictions of ground and support behavior should be quantified reliably based on data obtained by analysis and measurement, as in previous studies.

Against this background, this study develops a numerical analysis method using a DA technique that updates the numerical model based on measured data during construction. This method predicts the behavior of the excavated and unexcavated areas. The behavior prediction of excavated areas can be used to examine the necessity of countermeasures. The behavior prediction of unexcavated areas will contribute to the examination of support patterns. In general, computational models are developed based on idealized and simplified mathematical models of real phenomena, such as partial differential equations, initial and boundary conditions, and constitutive equations. For this reason, the computational models also include discretization errors, rounding errors. Therefore, they cannot perfectly reproduce the actual phenomena. On the other hand, DA is a technique that accounts for errors in the computational model and uses observed data to modify the model and improve performance. A probability distribution of the predicted result is acquired because parameter uncertainties are considered in DA. This is expected to quantify and improve the reliability of excavation analyses that deal with various uncertainties. A combination of excavation analysis and DA is outlined in this report. The results of numerical experiments simulating tunnel construction in the ground assuming a strain-softening model are also reported.

2 DATA ASSIMILATION FOR EXCAVATION ANALYSIS

There are various DA methods. In this study, we employed the Error Subspace Transform Kalman Filter (ESTKF), which is a sequential DA method as well as an ensemble-based DA method. The ESTKF is advantageous in terms of the relatively low computational cost. Below is an overview of the Ensemble Kalman Filter (EnKF) and its combination with the tunnel excavation analysis and DA. ESTKF is derived from EnKF. A detailed description of ESTKF has been omitted because of space limitations. In EnKF, the state-space model is first set up as follows:

$$\mathbf{x}_n^{\mathrm{FVM}} = \mathbf{f}(\mathbf{x}_{n-1}, \mathbf{v}_n) \tag{1}$$

$$\mathbf{y}_n = \mathbf{H}\mathbf{x}_n + \boldsymbol{\omega}_n \,, \boldsymbol{\omega}_n \sim N(0, \mathbf{R}) \tag{2}$$

x is a state vector consisting of state variables such as nodal displacements, element stresses, and ground properties; **v** is the system noise; the subscript FVM is the result of the finite volume method (FVM) analysis before DA (prior distribution); n is the construction step. **f** is an operator that expresses the time evolution of variables from construction step n-1 to n. This **f** corresponds to the excavation analysis by FVM using the commercial software FLAC3D. **y** is a vector consisting of the displacements caused by the excavation at the observation point (hereafter referred to as the observation vector), and **H** is the linear observation operator. **ω** is the observed noise following a normal distribution with mean 0 and covariance matrix **R**. The updating of state variables based on the observed data is performed by an EnKF, which is expressed as follows:

$$(\mathbf{x}_n^{\mathrm{DA}})_i = (\mathbf{x}_n^{\mathrm{FVM}})_i + \mathbf{K}_n[\mathbf{y}_n + \boldsymbol{\omega}_n - \mathbf{H}(\mathbf{x}_n^{\mathrm{FVM}})_i] \tag{3}$$

$$\mathbf{K}_n = \mathbf{P}_n\mathbf{H}^{\mathrm{T}}(\mathbf{H}\mathbf{P}_n\mathbf{H}^{\mathrm{T}} + \mathbf{R}_n)^{-1} \tag{4}$$

$$\mathbf{P}_n \approx \frac{1}{N-1}\sum_{i}^{N}[\{(\mathbf{x}_n)_i - \hat{\boldsymbol{x}}_{\boldsymbol{n}}\}\{(\mathbf{x}_n)_i - \hat{\boldsymbol{x}}_{\boldsymbol{n}}\}^{\mathrm{T}}] \tag{5}$$

The subscript i is the index of the ensemble member and DA is the posterior distribution after the update. **K** is the Kalman gain, $\mathbf{P}_n$ is the error covariance matrix, and N is the number of samples in the ensemble. $\hat{\boldsymbol{x}}_{\boldsymbol{n}}$ is the ensemble mean of the state vectors. In sequential DA, the simulation proceeds by repeated prediction using Equation (1) and updating using Equation (3). Figure 1 shows an overview of ground displacement prediction using this method. The left two figures show a schematic of the longitudinal section along the tunnel axis, with blue and yellow circles indicating the observation and prediction points for displacement, respectively. The upper longitudinal section shows the early stage of excavation with few observation points, and the lower section shows the stage when excavation has progressed and the number of observation points has increased. The graph below the longitudinal section shows the predicted cumulative displacement from the start of observation for the top two excavation steps. The horizontal axis represents the position of the tunnel face and the vertical axis represents the predicted displacement. The blue and red lines show the predicted results at the early and advanced stages of the excavation, respectively. Solid and dashed lines indicate the smallest and largest predicted values, respectively. This method quantitatively demonstrates the reliability of the prediction results as a probability distribution. Additionally, the prediction accuracy improves as the number of observation points increases.

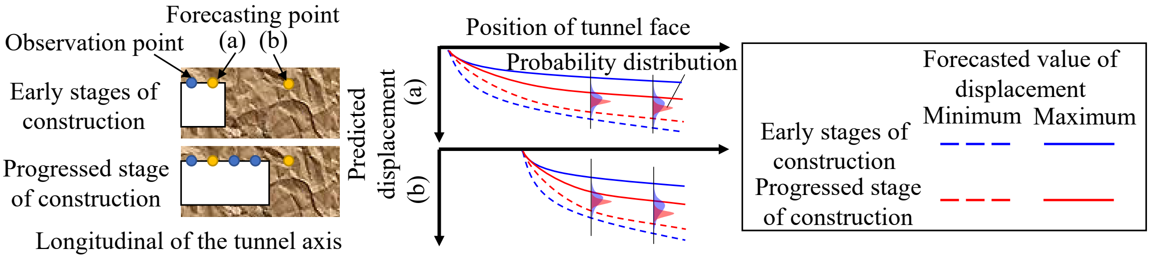

Figure 1. Overview of excavation analysis applying DA.

3 OVERVIEW OF NUMERICAL EXPERIMENTS

Numerical experiments simulating tunnel construction were conducted to confirm whether DA could provide an estimation of the physical properties of the ground by assuming a strain-softening model. In this numerical experiment, the results calculated by the analytical model under the correct condition were considered as the measurement data, and the measurement data were successively assimilated to the prediction results of the analytical model under different conditions from the correct value. This type of numerical experiment is commonly performed to examine whether DA correctly addresses the problem efficiently and whether the parameters can be estimated because the true values are known. In this study, the following points were examined: (i) How are the physical properties of the ground in the prediction model updated by DA? (ii) How will the predicted results of the ground displacement in the prediction model be changed?

Numerical experiments simulated a tunnel section construction of the Asahan Hydroelectric Power Plant Project in Indonesia. The analysis mesh and observed points of ground displacement are shown in Figure 2. To eliminate the influence of the boundary conditions on the ground displacement, the cross-sections of the observation points were established after a tunnel distance (TD) of 30m. To reduce the time required for excavation analysis in the numerical experiments, the observation cross-sections were spaced 2m apart from TD30m. DA was performed for every 2m of excavation in the section from TD30m to TD50m. In other words, 10 DA cycles was performed.

A strain-softening model was assumed for the analytical model of the ground because softening behavior was observed after yielding in the laboratory tests. Figure 3 shows an example of the relationship between cohesion c, friction angle ϕ, and plastic shear strain ε^{ps} in this model.

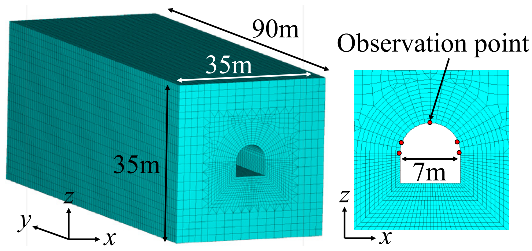

Figure 2. Numerical model for excavation analysis.

$$\Delta\varepsilon^{ps} = \frac{1}{\sqrt{2}}\sqrt{(\Delta\varepsilon_1^{ps}-\Delta\varepsilon_m^{ps})^2+(\Delta\varepsilon_2^{ps}-\Delta\varepsilon_m^{ps})^2+(\Delta\varepsilon_3^{ps}-\Delta\varepsilon_m^{ps})^2}$$

$$\Delta\varepsilon_m^{ps} = (\Delta\varepsilon_1^{ps}+\Delta\varepsilon_3^{ps})/3$$

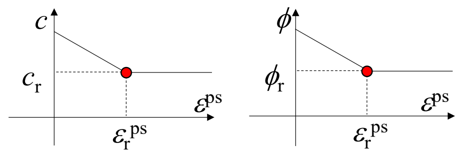

Figure 3. Relationship between c_r, ϕ_r and ε^{ps}.

The behavior during softening was reproduced by decreasing c and ϕ as ε^{ps} increased. ε_r^{ps} is the plastic shear strain at the change from softening behavior to residual.

The initial stresses in the analytical model were set by referring to the results of the in-situ tests (σ_{xx} = 6.68MPa, σ_{yy} = 3.10MPa, σ_{zz} = 6.40MPa, τ_{xy} = 2.57MPa, τ_{yz} = 1.38, τ_{zx} = -0.99MPa). After performing the initial stress analysis considering gravity and unit volume weight, the initial stress components obtained from the in-situ tests were added to all elements. Table 1 lists the physical properties of the ground obtained from the in-situ tests and used in the numerical experiments.

Table 1. Physical properties of the ground.

	ϕ(°)	ϕ_r(°)	c(MPa)	c_r(MPa)
In-situ test result	50	45	2.78	1.0
Correct value in analysis Case 1	40	36	2.22	0.8
Correct value in analysis Case 2	30	27	1.67	0.6

c_r and ϕ_r are the cohesion and friction angle of the ground in the residual state, respectively. The deformation modulus E and Poisson's ratio v obtained by in-situ tests were 2390MPa and 0.2, respectively. These values of E and v were used for the analysis of Cases 1 and 2. ε_r^{ps} was set to 0.008 based on the laboratory test results. The tensile strength σ_t was set to the value at the intersection of σ axis and the failure line estimated from c and ϕ. A plastic zone did not appear when the tunnel excavation analysis was performed using the properties obtained from the in-situ tests. Therefore, even if these analysis results were used as observed values for DA, it would not be possible to estimate properties other than the deformation modulus. Therefore, we reduced the values of the physical properties, as shown in Analysis Cases 1 and 2 in Table 1, such that the plastic region would appear.

Figure 4 shows the relationship between the position of the tunnel face and ε^{ps} of the top and sidewall elements near the tunnel at TD30 m in Cases 1 and 2. In Case 1, ε^{ps} is smaller than ε_r^{ps} and the values of c and ϕ of the yielding element do not decrease to c_r and ϕ_r. However, in Case 2, ε^{ps} of the element is larger than ε_r^{ps}, and c and ϕ of the yielding element decrease to c_r and ϕ_r. In both cases, the occurrence of the plastic region is not bilaterally symmetrical with respect to the central axis of the tunnel because of the influence of the initial stress.

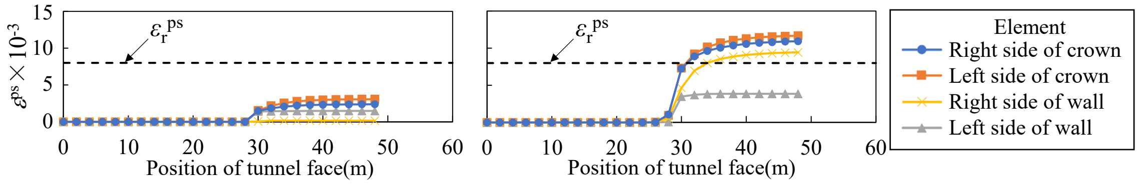

(i) Case 1 (ii) Case 2

Figure 4. Relationship between the position of tunnel face and ε^{ps} of the elements near the tunnel at TD30m.

The following is a numerical experiment procedure. In Step 1, an excavation analysis was performed under the correct conditions to produce simulated observed values (observation vectors) of the ground displacement. In Step 2, the state vector was created by performing excavation analysis up to excavation step n using an ensemble of multiple conditions. The initial distribution of the properties for the ensemble was obtained from the ranges shown in Table 2 by uniform random numbers.

Table 2. Range for obtaining the initial distribution of the ensemble.

E(MPa)	c(MPa)	c_r(MPa)	ϕ (°)	ϕ_r(°)	ε_r^{ps}
500-5000	0-6	0-c_{ens}	15-65	0-ϕ_{ens}	0-0.015

Subscript "ens" indicates the ensemble value. $c_{r,ens}$ and $\phi_{r,ens}$ are obtained from a range smaller than c_{ens} and ϕ_{ens} because of the assumption of the strain-softening model. In Step 3, the observed displacement calculated using the correct conditions and the ensemble excavation analysis were assimilated, and the six parameters shown in Table 2 were updated. To assume a strain-softening model, if the updated parameters were not realistic (e.g., negative values, $c_r^{DA} > c^{DA}$, $\phi_r^{DA} > \phi^{DA}$), the parameter values were obtained from the ranges presented in Table 2. DA generally reduces the parameter variation. If the variance of the distribution after updating is exceedingly small, the physical properties do not change significantly during the subsequent DA. Therefore, noise of -10 to 10% of the ensemble mean was added to each parameter after updating, and excavation analysis was performed up to excavation step n+1. In a previous study, to satisfy the physical relationship between the ground properties and nodal displacements, the authors used the method of returning to a specific excavation stage, adding the ground parameters after DA to the analytical model, and subsequently reperformed the excavation analysis. The numerical experiments were conducted using this method. To verify whether DA can theoretically estimate the physical properties of the ground assuming a strain-softening model, the observation error of the ground displacement was set to an extremely small value of 2.0×10^{-2}mm. The observation noise was not considered in this numerical experiment.

4 RESULT

4.1 Estimation of ground properties

Figure 6 shows the results before and after each assimilation step of the ground properties in analysis Cases 1 and 2. In this figure, the black lines represent the correct values, the blue round symbols represent the distribution of the properties used in the excavation analysis for each step, and the orange triangular symbols represent the distribution after the update. Figure 6 shows that DA reduced the variation in the ground properties in both Cases 1 and 2. In Case 1, the distributions of properties other than c_r and ϕ_r converged to the correct values. The values of c_r and ϕ_r converged to larger and smaller values, respectively than the correct values. In Case 1, because the ε^{ps} of the yielding element was smaller than the correct ε_r^{ps} as shown in Figure 4, c and ϕ of the yielding element did not decrease to c_r and ϕ_r, respectively, as shown in Figure 3. Furthermore, in Case 2, the distributions of all properties, including c_r and ϕ_r, converged to the correct values. In Case 2, ε^{ps} of the elements around the tunnel were larger than ε_r^{ps}, as shown in Figure 4. Because this assimilation was performed using the displacements in the residual state, all properties were able to converge to the correct values.

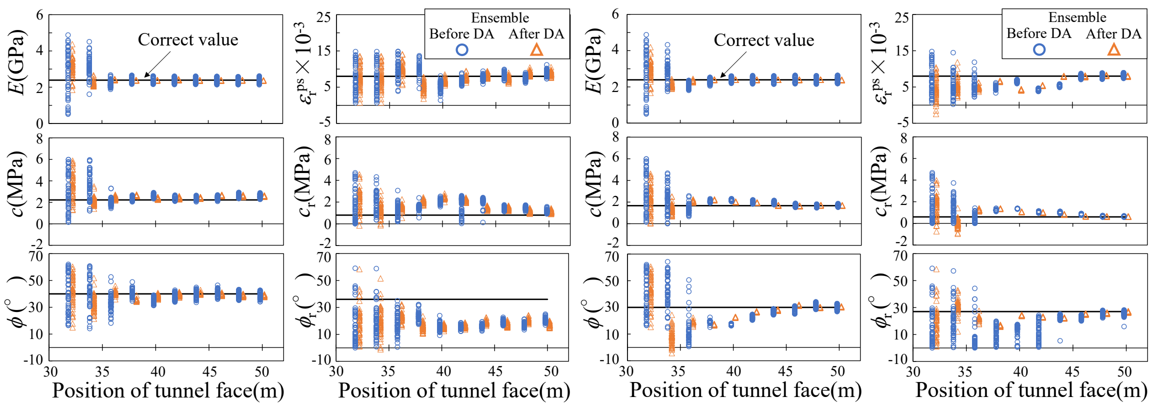

(i) Case 1 (ii) Case 2

Figure 6. Distribution of the physical properties before and after performing 10 DA cycles.

4.2 Prediction of ground displacement

Figure 7 shows the relationship between the position of the tunnel face and the settlement of the crown at 60m before and after performing 10 DA cycles. The vertical axis represents this settlement in terms of absolute displacement. The black line indicates the settlement calculated using the correct condition. The blue and orange lines show the settlement calculated using the initial ensemble before performing DA and the ensemble after performing 10 DA cycles. Before DA, the settlement could not be accurately predicted because of the large variation in the physical properties. However, DA improved the settlement prediction because the physical properties of the ground converge to the correct solution. In Case 2, in which the c and ϕ of the elements near the tunnel excavation surface decrease to c_r and ϕ_r, the parameters of the strain softening model (Figure 3, 4) can be estimated accurately after 10 DA cycles, resulting in a small prediction error of the crown settlement. On the other hand, in Case 1, in which the c and ϕ of the elements near the tunnel excavation surface do not decrease to c_r or ϕ_r near the tunnel excavation surface (Figure 3, 4), c_r and ϕ_r do not agree with the correct value as much as in Case 2 (Figure 6). This result shows the effectiveness of the model as a prediction model of crown settlement by estimating a plausible value as a combination of the c_r - ε^{ps} relationship and the ϕ_r - ε^{ps} relationship. However, it does not estimate the complexity of the mechanical model that explains the mechanism of residual behavior because there is no observation data that reach the residual state in Case 1.

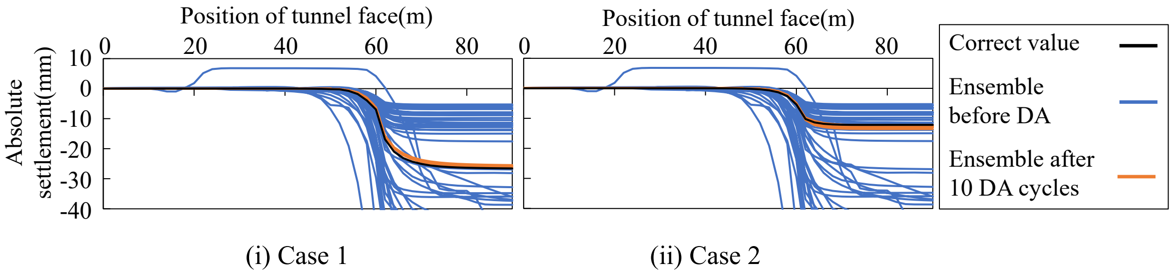

Figure 7. Predicted crown settlement at TD60m before and after performing 10 DA cycles.

5 CONCLUSION

The excavation analysis that applies DA techniques was introduced. Subsequently, numerical experiments were conducted to confirm that the parameters and displacements of the ground, assuming the strain-softening model, can be estimated by DA. The numerical experiments assimilated the displacement of the excavation surface, which exhibited an extremely small observation error. In the case which observed data that does not reach the residual state is used for DA, the effectiveness is shown as a predictive model of crown settlement, but it does not estimate the complexity of the mechanical model that explains the mechanism of residual behavior. On the other hand, in the case which the observed data that reaches the residual state is used for DA, the model is updated to have appropriate performance as the prediction model and the mechanical model as well. Although a homogeneous analytical model was used in this numerical experiment, the modeling of geological heterogeneity must be investigated further. Future research should examine approaches to resolve these issues.

REFERENCES

Shuku, T., Nishimura, S., Murakami, A., Nishimura, Y., & Fujisawa, K. 2011. Performance verification for geotechnical structures using reliability analysis based on data assimilation: Japanese Geotechnical Journal 6(3), pp.415-426.

Nerger, L., Janjić, T., Schröter, J., & Hiller, W. 2021. A unification of ensemble square root Kalman filters: Monthly Weather Review, pp.2335-2345.

Evensen, G. 1994: Sequential data assimilation with a nonlinear quasi-geostrophic model using Monte Carlo methods to forecast error statistics: Journal of Geophysical Research 99(5), pp.10143-10162.

Varas, F., Alonso, E., Alejano, L.R., & Fdez.-Manı´n, G. 2005. Study of bifurcation in the problem of unloading a circular excavation in a strain-softening material: Tunnelling and Underground Space Technology 20, pp.311-322.